Chemical and Thermophysical Characterization of an Algae-Based Hydrotreated Renewable Diesel Fuel

Peter Y. Hsieh, Jason A. Widegren, Tara J. Fortin, and Thomas J. Bruno*

National Institute of Standards and Technology, Material Measurement Laboratory Applied Chemicals and Materials Division, 325 Broadway, MS 647.07, Boulder, Colorado 80305, United States

Ⓢ Supporting Information

ABSTRACT: Second-generation renewable fuels are synthesized through biochemical and thermochemical processes from nonfood biomass feedstock. The resultant fuels are similar to aliphatic synthetic fuels produced through the Fischer−Tropsch process, which contain mainly linear and lightly branched alkanes. We applied the advanced distillation curve method to an algae-based hydrotreated renewable naval distillate fuel (HRD-76) to measure its boiling temperature as a function of distillate volume fraction. Analysis of the bulk fuel sample through nuclear magnetic resonance spectroscopy, gas chromatography, and mass spectrometry showed the principal components to be linear and branched alkanes containing 14−18 carbon atoms. The speed of sound and density of the fuel were estimated from its composition and compared with experimental data measured with a density and sound speed analyzer. The estimates were within 5% of the experimental values. The boiling temperature, density, and composition data were used to estimate the calculated cetane index of the fuel. We also measured the cloud point of the fuel through a constant cooling rate method with optical detection of paraffin wax precipitation. The measured cloud point was consistent with reported values for hydrotreated renewable fuels, which tend to be higher than cloud points of diesel fuels derived from petroleum. The quantitative thermophysical and chemical data can be used to improve combustion modeling of HRD-76 and other second-generation renewable fuels.

1. INTRODUCTION

Renewable fuels have attracted considerable interest in recent years due to the rising cost of petroleum. First-generation renewable fuels, such as bioethanol and fatty acid methyl esters (FAMEs), are often blended with petroleum distillate fuels for use in motor vehicles.[1] The diversion of food crops to first-generation renewable fuel production has proven to be a controversial issue;[2,3] moreover, corrosion of metallic parts in engines[4] and long-term stability[5,6] have been identified as potential problems for renewable fuel blends. The short-comings of first-generation renewable fuels have prompted research into new approaches that address these concerns.

Second-generation renewable fuels, or advanced biofuels, are produced from nonfood biomass such as agricultural by-products and microalgae.[3,7] Microalgae, including diatoms and green algae, are photosynthetic microorganisms capable of capturing energy from sunlight and storing it as lipid compounds. They are attractive for energy production because of their high biomass productivity and their ability to grow in brackish or saline environments.[8] Cultivation of microalgae does not compete with food crops for land and resources. Oil from microalgae can be converted to chemically stable and energy-dense diesel fuels through hydrotreatment, a chemical process where the algal oil reacts with hot pressurized hydrogen gas in the presence of catalysts to remove oxygen-containing functional groups and to hydrogenate unsaturated olefinic compounds.[9,10]

The main components of hydrotreated algal oil are linear alkanes or *n*-paraffins, principally heptadecane and octadecane with smaller amounts of pentadecane and hexadecane; other *n*-alkanes are present in trace quantities.[10] The distribution of the *n*-alkanes reflects the fatty acid profile of the algal oil. The C_{15} to C_{18} linear alkanes have notably high cetane numbers (ranging from 95 to 105), a measure of compression ignition quality in diesel engines.[11] Diesel fuels with low cetane numbers combust prematurely, resulting in poor engine performance. Though the high *n*-alkane content of hydro-treated algal oil is favorable in boosting the cetane number of diesel fuel blends, it can result in unfavorable low-temperature fuel properties. The same *n*-alkanes increase the pour point, cloud point, and cold filter clogging point in diesel fuels.[12] These low-temperature fuel properties may be improved through catalytic hydroisomerization, by converting some of the *n*-alkanes to branched alkanes or isoparaffins.[13] A balance between the fuel ignition quality and the low-temperature properties is attained by controlling the extent of branched alkane formation during hydroisomerization.

Changes in the chemical composition and physical properties of renewable diesel fuel blends can produce significant changes in the atomization and combustion of the fuel, as well as the engine emissions profile.[14] The chemical composition and physical properties of second-generation renewable fuels are different from conventional petroleum distillate fuels or first-generation FAME-based biodiesel fuels. Chemically, algae-based hydrotreated renewable diesel fuel is similar to synthetic fuels produced through the Fischer−Tropsch (F-T) process in that both contain principally linear and branched alkanes.[15] Unlike petroleum distillate fuels, neither the algae-based

hydrotreated renewable diesel fuel nor F-T synthetic fuels contain significant amounts of aromatic or cycloalkane (naphthenic) compounds. Characterizing the chemical and physical properties of second-generation renewable fuels is important in formulating diesel fuel blends that are compatible with engines and fuel distribution infrastructure in use today.

Smagala et al. and Prak et al. have characterized many properties of algae-based hydrotreated renewable diesel fuel, including density, speed of sound, viscosity, surface tension, enthalpy of combustion, cetane number, and cloud point.[9,16] These bulk fluid values are significant in establishing an equation of state for modeling the vaporization and combustion of algae-based hydrotreated renewable diesel fuel droplets. As the liquid droplet vaporizes, its chemical composition and physical properties change as a function of time. By measuring the changes in the fuel composition over its boiling temperature range, it is possible to estimate changes in these parameters and improve the fidelity of fuel droplet combustion models.

The advanced distillation curve (ADC) method offers significant advantages over earlier approaches to complex fluid characterization, featuring (1) a composition-explicit data channel for each distillate fraction (for both qualitative and quantitative analyses), (2) temperature, volume, and pressure measurements of low uncertainty that are true thermodynamic state points suitable for equation of state development, (3) consistency with a century of historical data, (4) an assessment of the density and enthalpy as a function of distillate volume fraction, (5) trace chemical analysis of each distillate fraction, and (6) a corrosivity assessment of each distillate fraction.[17−19] It has been used to characterize n-alkanes,[20] simple azeotropes,[21] gas turbine fuels,[22−27] diesel and biodiesel fuels,[28−34] gasolines,[35−37] rocket propellants,[22,38−40] and crude oils.[41−44] Unlike the conventional distillation curve, fuel volatility or vapor−liquid equilibrium data, ADC data can be modeled with an equation of state.[45−50] We applied the ADC method and other analytical techniques to the analysis of algae-based hydrotreated renewable diesel fuel in order to expand the physical and chemical data suitable for detailed modeling of the vaporization and combustion of second-generation renewable fuels in diesel engines. Indeed, the major application of the ADC method is to provide the infrastructure for thermophysical property models based on the Helmholtz free energy equation of state.[46−54]

2. MATERIALS AND METHODS

2.1. Materials. A sample of algae-based hydrotreated renewable diesel fuel (lot number 12119-04718-000) was provided by the Naval Fuels and Lubricants Cross Function Team at Patuxent River, Maryland. The HRD-76 fuel was produced from algae grown in environmentally controlled reaction vessels; the algal oil was processed with a two-stage hydrotreatment method using proprietary catalysts. The sample was measured and analyzed as received. We note that the focus of the present work is on the chemical and thermophysical characterization of the as-received fuel, not its synthesis. We further note that the nomenclature HRD-76 is consistent with usage in the renewable fuels literature to describe hydrotreated renewable diesel fuel suitable for use in place of NATO F-76 naval distillate/diesel fuel. The n-hexane solvent used in gas chromatography was purchased from a commercial supplier and determined to be approximately 99% (mass/mass) pure through gas chromatography with mass spectrometric detection (GC-MS). Deuterated chloroform (CDCl$_3$) with a stated minimum isotopic purity of 99.8% used in the nuclear magnetic resonance (NMR) spectroscopy analysis was also purchased from a commercial supplier. The CDCl$_3$ was used without further purification.

2.2. Advanced Distillation Curve Method. The reduced-pressure ADC apparatus and sampling method have been described in detail in earlier works;[20,22,24,35,55] a limited description of the particular steps used in this study is reported here for clarity. The boiling flask (kettle) was filled with 100 mL of HRD-76 fuel from a volumetric pipet. The mass of the HRD-76 fuel was then measured on an analytical balance. Two thermocouples were inserted into the distillation head and boiling flask to monitor the vapor temperature at the bottom of the distillate takeoff position (T_h) and the liquid temperature in the kettle (T_k). An aluminum heating enclosure was used to increase the fluid temperature uniformly and at a constant rate. The sample temperature was raised slowly under manual control, using prior distillation data as a guide for the ramp rate. The distillation was performed at ambient pressure (83 kPa in Boulder, Colorado, USA). Pressure measurements were made concurrently during distillation with an electronic barometer. The reduced-pressure ADC apparatus is effectively a closed system for mass transfer when operated at ambient pressure, simplifying analysis of the resultant data. A calibrated volume graduated receiver was used to measure the distillate volume.

2.3. Gas Chromatography with Mass Spectrometric Detection (GC-MS). Small aliquots (10 μL) of the distillate were withdrawn at predetermined distillate volume intervals with a standard chromatography syringe in the receiver adapter hammock. The aliquots were dissolved in a fixed quantity of n-hexane (approximately 1 mL) inside an autosampler vial. The diluted aliquots were analyzed through temperature-programmed gas chromatography (30 m column with a 250 μm film of 5% phenyl−95% dimethylpolysiloxane, with helium carrier gas at 48 kPa or 7 psi inlet pressure, a split ratio of 1.17:1, and a temperature program starting at 75 °C for 2 min followed by a fast ramp-up to 300 °C at a heating rate of 3 °C/min).[56] Mass spectrometric detection was used to identify and quantify compounds present in the distillate. The n-alkanes present in the sample were used as internal standards to calculate programmed-temperature retention indices as a function of absolute retention time (see Supporting Information, section S1, for additional details). These values were used to narrow down candidate compounds in conjunction with mass fragmentation pattern data from the NIST 11 Mass Spectral Library to improve peak identification.[57] Bulk HRD-76 fuel was also analyzed using a slower heating rate (starting at 75 °C for 3 min, followed by a slow ramp-up to 225 °C at 1 °C/min) to improve the resolution of higher molecular mass peaks.

2.4. Nuclear Magnetic Resonance (NMR) Spectroscopy. The HRD-76 fuel was analyzed by both ^{1}H and ^{13}C NMR spectroscopy. A sample for ^{1}H NMR spectroscopy was prepared by dissolving 20 mg of the fuel in 1 g of CDCl$_3$. A sample for ^{13}C NMR spectroscopy was prepared by dissolving 200 mg of the HRD-76 fuel in 1 g of CDCl$_3$. We used a commercial 600 MHz NMR spectrometer with a cryoprobe, operated at 150.9 MHz for ^{13}C, to obtain the spectra. The samples were maintained at 30 °C for all of the NMR measurements. Spectra were referenced to the solvent peak (7.23 ppm for ^{1}H and 77.0 ppm for ^{13}C).

A quantitative ^{1}H NMR spectrum was obtained with a 30° flip angle and a long interpulse delay (9.1 s acquisition time, 10 s relaxation delay). A sweep width of 6,009.62 Hz (0 ppm to 10 ppm) was used. After 64 scans the spectrum had a signal-to-noise ratio of about 1.4×10^5.

A quantitative ^{13}C NMR spectrum was obtained by use of inverse-gated waltz proton decoupling and a long interpulse delay (2.17 s acquisition time, 40 s relaxation delay). A sweep width of 15 121 Hz (−10 ppm to 90 ppm) was used for a total of 1024 scans. The peaks in this spectrum were integrated to determine the relative abundance of CH, CH$_2$, and CH$_3$ carbons. Peak assignments were made by comparing this spectrum with the spectra obtained from ^{13}C distortionless enhancement by polarization transfer (DEPT)-90 and ^{13}C DEPT-135 experiments, the former giving peaks only from CH groups (90° selection angle parameter, or the tip angle of the final ^{1}H pulse), and the latter giving all CH and CH$_3$ carbons in a phase opposed to CH$_2$ carbons (135° selection angle parameter). For both DEPT experiments, a coupling constant ($J_{C−H}$) of 125 Hz was used because the sample contains mostly linear and branched alkanes.[58] A

Table 1. Primary, Secondary, and Tertiary Carbon Distribution of HRD-76 Fuel Determined by ^{13}C NMR and GC-MS^a

	^{13}C NMR, %	U_c	GC-MS, %	U_c	^{13}C NMR hydrotreated algal oil,[9] %	^{13}C NMR hydrotreated vegetable oil,[9] %
CH$_3$ (primary)	19.9	1.1	19.1	0.2	16.4	17.8
CH$_2$ (secondary)	72.0	2.3	74.2	0.3	73.4	74.9
CH (tertiary)	8.1	0.7	6.7	0.1	9.9	7.3
n-alkane			31.3	0.2	26.8	31.4
isoalkane			68.7	2.0	70.9	66.0

^{a}Combined expanded uncertainty (U_c) values with a coverage factor of 2 are shown to the right of their respective measured values. See text for discussion of uncertainty in measurement results.

sweep width of 15,121 Hz (−10 ppm to 90 ppm) was used. Other acquisition parameters for the DEPT experiments included an acquisition time of 2.17 s, a relaxation delay of 10 s, and a total of 256 scans.

Three sources of uncertainty were considered for the integration of peaks in the quantitative ^{13}C spectrum: peak overlap, incomplete relaxation, and baseline drift. By our estimation, the largest source of uncertainty was peak overlap, which was particularly problematic for the CH carbon peaks. Estimated values for the three sources of uncertainty were added in quadrature to arrive at the combined expanded uncertainties that are reported in the Results and Discussion.

2.5. Density and Speed of Sound Analysis. A commercial density (ρ) and speed of sound (w) analyzer was used to simultaneously measure these two properties for the HRD-76 fuel over the temperature range of 5−70 °C and at ambient pressure (approximately 83 kPa). Details of the instrument, experimental procedures, and uncertainty analysis have been previously reported;[59,60] therefore, only a limited description will be provided here. The instrument contains a time-of-flight sound speed cell and a quartz vibrating tube densimeter connected in series. Both measurement cells are housed in a copper block whose temperature is controlled with a combination of thermoelectric Peltier elements and a platinum resistance thermometer. The parameters of the instrument's working equation are adjusted via measurements of air and water at 20 °C, 40 °C, and 60 °C. Additionally, the instrument's performance is checked before and after sample measurements via calibration measurements of water and toluene standard reference material (SRM) 211d performed over the full temperature range of the instrument.[61] For the HRD-76 fuel measurements, programmed temperature scans were performed from 70 to 5 °C in 5 °C decrements. The samples were injected at room temperature and allowed to reach thermal equilibrium in the instrument. A fresh aliquot of sample was injected into the instrument prior to each temperature scan, and a total of five separate injections/scans were performed.

2.6. Cloud Point Measurement. A modified constant cooling rate test method (ASTM D5773) was used to measure the cloud point, or wax appearance temperature, of the HRD-76 fuel.[62] A volumetric pipet was used to deliver 150 μL of the fuel into an aluminum specimen cup. The sample was air-cooled at a constant rate of −1.4 °C/min with an expanded uncertainty of 0.1 °C/min in a temperature-controlled test chamber while being illuminated by a monochromatic fiber-optic light source (λ = 660 nm). The reflected light intensity was measured with a single-mode optical fiber coupled to a photodiode power sensor. The cloud point is determined by calculating the temperature at which the scattered light intensity increases from the baseline. The temperature was measured to 0.1 °C resolution with a K-type thermocouple immersed in the fuel sample.

3. RESULTS AND DISCUSSION

3.1. NMR and GC-MS Analyses of Bulk HRD-76 Fuel Composition. NMR spectroscopy is widely used for the study of hydrocarbon fuels because it simultaneously provides information about the chemical structures and the relative concentrations of individual fuel components.[58] The HRD-76 fuel is especially amenable to NMR analysis in that it consists almost entirely of saturated or aliphatic hydrocarbons with no quaternary branching. In this type of sample, it is possible to

calculate the extent of branching and the average molecular mass with no assumptions.

First, we obtained a quantitative ^{1}H spectrum for the HRD-76 fuel with a high signal-to-noise ratio in order to check for the presence of aromatic, oxygenated, and alkene (olefinic) compounds. Ignoring the NMR solvent peak, only very small resonances were observed outside of the aliphatic range (from 0.0 to 2.0 ppm). The combined intensity of these minor peaks was approximately 0.1% of the total. These low-intensity peaks were grouped into two regions of the spectrum. One group occupied the spectral region between 6.5 and 7.5 ppm, and the other group occupied the spectral region between 2.0 and 3.5 ppm, which indicates that these minor impurities are likely aromatic and oxygenated compounds. The absence of any peaks in the range from 4 to 6 ppm shows that the alkene content of the fuel is below the detection threshold of the experiment (<0.01% olefinic protons).[56] The concentrations of these trace components are too low to significantly affect the calculations that follow.

Next, we collected three ^{13}C NMR spectra. First, a quantitative ^{13}C NMR spectrum was obtained by use of inverse-gated waltz proton decoupling and a long interpulse delay. Then ^{13}C DEPT-90 and ^{13}C DEPT-135 spectra were obtained, which allows one to determine the number of protons attached to each type of carbon. The peaks in the quantitative ^{13}C NMR spectrum were assigned by comparison with the ^{13}C DEPT-90 and ^{13}C DEPT-135 spectra. Then the quantitative ^{13}C NMR spectrum was integrated to give the relative abundance of CH, CH$_2$, and CH$_3$ carbons. The values obtained, along with the combined expanded uncertainty with a coverage factor (k) of 2 in parentheses, were 19.9(1.1)% CH$_3$ carbons, 72.0(2.3)% CH$_2$ carbons, and 8.10(0.67)% CH carbons (see Table 1). There was no evidence of quaternary carbons in the ^{13}C NMR spectra; however, it is difficult to estimate an upper limit for the abundance of quaternary carbons because of the potential for peak overlap.

For saturated hydrocarbons with no quaternary branching, the average number of branch points per molecule is readily determined from the ratio of CH to CH$_3$ carbons. For example, a single branch alkane (methylalkane) will have three CH$_3$ carbons and one CH carbon (for a CH/CH$_3$ ratio of 1/3), a double branch alkane (dimethylalkane) will have four CH$_3$ carbons and two CH carbons (for a CH/CH$_3$ ratio of 1/2), and so forth. The ratio of CH/CH$_3$ in the HRD-76 fuel can be shown to correspond to an average of 1.4 branches per molecule with an expanded (k = 2) uncertainty of 0.3 branches per molecule.

The average molecular mass can be determined from the relative abundance of CH, CH$_2$ and CH$_3$ carbons. First, the average number of CH$_2$ groups per molecule was calculated from the equation
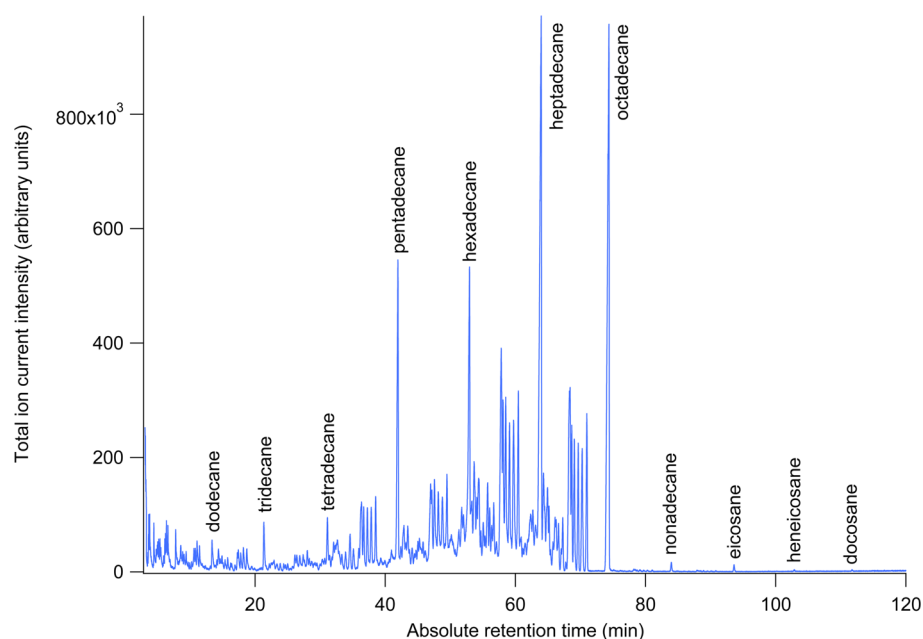
Figure 1. Representative total ion chromatogram of bulk HRD-76 fuel. Select *n*-alkane peaks identified through mass spectrometry useful as internal standards for calculating programmed-temperature retention indices are annotated in the figure.

$$N_{CH_2} = (2A_{CH_2})/(A_{CH_3} - A_{CH}) \qquad (1)$$

where A_{CH_2} is the relative abundance of CH_2 carbons (72.0% in this case), A_{CH_3} is the relative abundance of CH_3 carbons, and A_{CH} is the relative abundance of CH carbons. Then one adds two CH_3 end groups for each molecule, along with one CH and one CH_3 group for each branch point (there is an average of 1.4 branch points per molecule for the HRD-76 fuel). In this way, one can show that the average molecule in the HRD-76 fuel has 17 carbon atoms (i.e., the molecular formula is $C_{17}H_{36}$) with an expanded ($k = 2$) uncertainty of 2 carbon atoms. The branching density and average molecular mass derived from NMR data are substantially consistent with data obtained through GC-MS analysis of the bulk HRD-76 fuel, as described below.

GC-MS analysis is commonly used in the petroleum industry to characterize the composition of distillate fuels.[63] Compounds present in a sample are separated by the strength of their interaction with the chromatographic column and ionized in the mass spectrometer to produce characteristic molecular ion fragmentation patterns. Figure 1 shows the total ion current intensity as a function of absolute retention time for bulk HRD-76 fuel. Mass spectrometry was used to identify the *n*-alkane peaks present in the chromatogram. The relative retention times of the *n*-alkane peaks were then used to calculate the programmed-temperature retention indices of the isoalkane peaks. By combining the programmed-temperature retention index with molecular ion fragmentation patterns, we were able to identify most of the single branch alkanes. Due to the large number of isomers and potential for overlapping peaks for double or higher branch alkanes, we were unable to resolve the identity of the remaining peaks by use of the same approach.

Where peaks overlap, as is the case for most of the double branch alkanes, a multipeak fitting algorithm is used to estimate the contribution of each peak. Where the double branch alkane overlaps with one of the *n*-alkane peaks, its contribution to the signal is estimated from the area under its two nearest neighbor double branch peaks. The balance of the signal is assigned to

the *n*-alkane peak. The uncertainty in the peak area is less significant than the uncertainty introduced by unresolved peak overlap from double branch peaks and *n*-alkane peaks. Table 1 summarizes the relative abundance of CH, CH_2, and CH_3 carbons as measured with ^{13}C NMR and GC-MS in this study, along with literature data on hydrotreated algal and vegetable oils.[9] The ^{13}C NMR and GC-MS data in this study are in good agreement and are close to the values reported for hydrotreated algal oil and hydrotreated vegetable oil by Smagala et al.[9]

3.2. Density, Speed of Sound and Bulk Modulus of Bulk HRD-76 Fuel. Table 2 lists values of density and speed of sound obtained with the density and sound speed analyzer over the temperature range 5−70 °C at ambient pressure. Included

Table 2. Density (ρ), Speed of Sound (w), and Derived Values of Isentropic Compressibility (κ_s) of HRD-76 Fuel Measured in the Density and Sound Speed Analyzer As a Function of Temperature (T)[a]

T, °C	ρ, kg/m³	$U_c(\rho)$, kg/m³	w, m/s	$U_c(w)$, m/s	κ_s, TPa⁻¹	$U_c(\kappa_s)$, TPa⁻¹
5.00	787.28	0.34	1399.7	1.2	648.3	0.6
10.00	783.83	0.32	1380.1	1.2	669.8	0.6
15.00	780.38	0.31	1360.9	1.2	691.9	0.7
20.00	776.93	0.30	1341.8	1.2	714.9	0.7
25.00	773.49	0.29	1322.9	1.2	738.8	0.7
30.00	770.04	0.28	1304.1	1.2	763.6	0.8
35.00	766.58	0.27	1285.6	1.2	789.3	0.8
40.00	763.12	0.26	1267.2	1.2	816.1	0.8
45.00	759.66	0.24	1248.9	1.2	843.9	0.9
50.00	756.16	0.21	1230.9	1.2	872.9	0.9
55.00	752.68	0.21	1213.0	1.2	903.0	1.0
60.00	749.21	0.21	1195.3	1.2	934.2	1.0
65.00	745.73	0.21	1177.8	1.2	966.6	1.0
70.00	742.26	0.21	1160.7	1.2	1000.0	1.1

[a]The ambient pressure during the measurements was approximately 83 kPa.
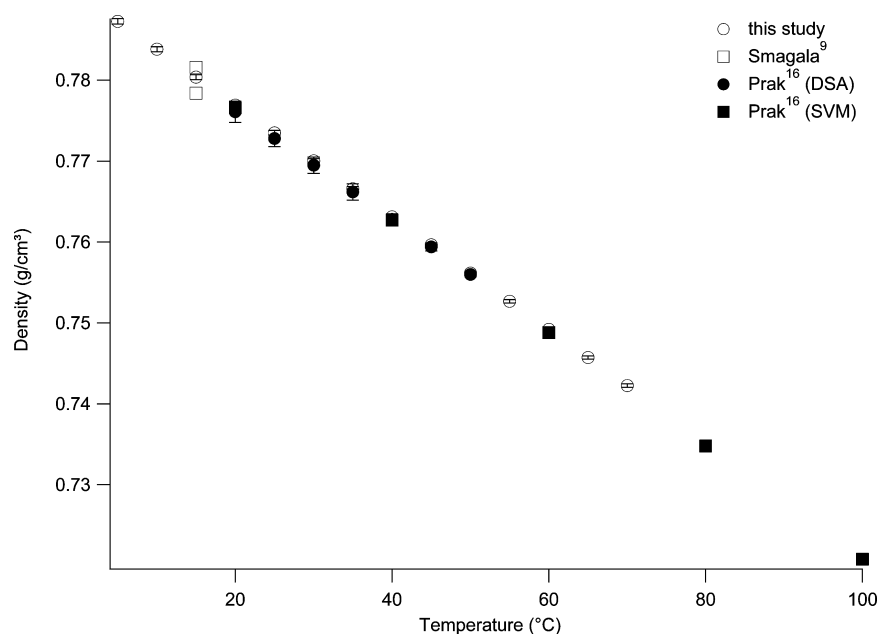
Figure 2. Density of HRD-76 fuel as a function of temperature: ○, this study; □, Smagala et al.;[9] ●, Prak et al.[16] (DSA, density and speed of sound analyzer); ■, Prak et al.[16] (SVM, Stabinger viscometer). The uncertainty values for density and temperature are smaller than the plotting symbols, as discussed in the text.
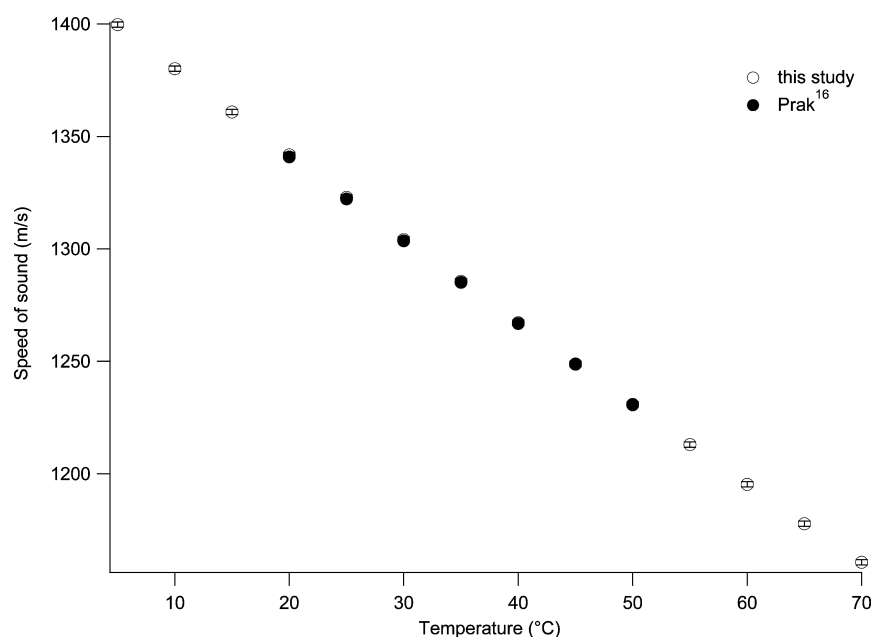

Figure 3. Speed of sound in HRD-76 fuel as a function of temperature: ○, this study; ●, Prak et al.[16] The uncertainty values for speed of sound and temperature are smaller than the plotting symbols, as discussed in the text.

in the table are averaged values for the five replicate measurement scans performed and their associated expanded uncertainty estimates, $U(\rho)$ and $U(w)$ for density and speed of sound, respectively. Expanded uncertainties were calculated using the expression

$$U(\rho) = t_\mathrm{p}(\mathrm{d}f_\rho)u(\rho) \tag{2}$$

where $t_\mathrm{p}(\mathrm{d}f_\rho)$ is taken from the t-distribution for $\mathrm{d}f_\rho$ degrees of freedom and a p percent level of confidence and $u(\rho)$ is the combined standard uncertainty for the averaged density measurements. Analogous calculations were performed for the speed of sound measurements. Additional details regarding the

calculation of the combined standard uncertainties and their associated degrees of freedom can be found in Fortin et al.[59] For both density and speed of sound, $t_\mathrm{p}(\mathrm{d}f_\rho)$ values corresponding to a 95% confidence level were used to calculate the reported expanded uncertainties. Those values ranged from 2.024 to 2.179 for density and from 2.023 to 2.028 for speed of sound.

Also included in Table 2 are derived adiabatic compressibilities (κ_s) calculated via the thermodynamic relationship

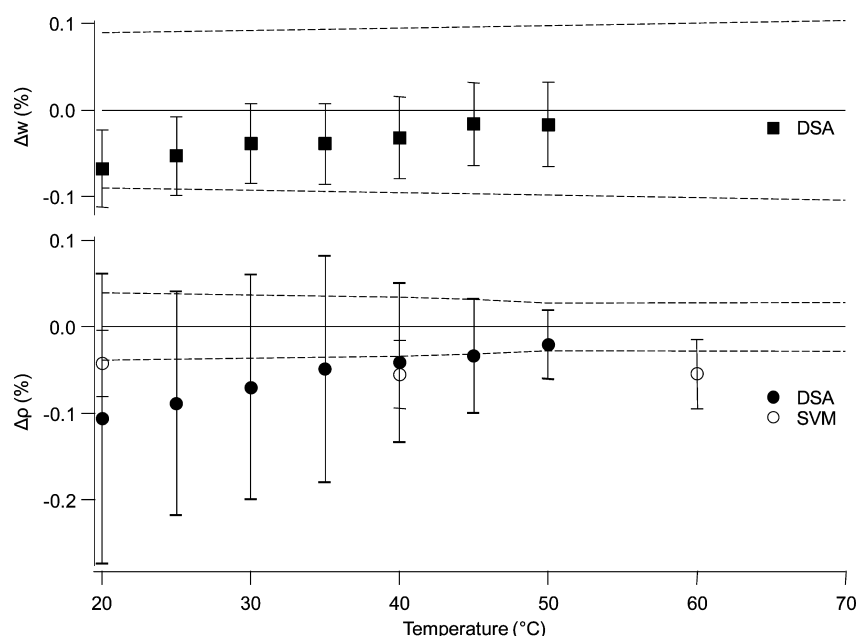$$\kappa_\mathrm{s} = (\rho w^2)^{-1} \tag{3}$$

Figure 4. Relative deviations (Δ) between this study, shown as a solid line (—) and Prak et al.[16] for measured values of density (ρ) and speed of sound (w) as a function of temperature. Densities measured by Prak et al.[16] using a Stabinger viscometer (SVM) are marked with open circles (O). Dashed lines (--) show the expanded uncertainty of this study's measurements at the 95% confidence level; error bars show expanded uncertainties reported by Prak et al.[16]

where ρ is density, w is speed of sound, and the subscript s indicates "at constant entropy". Expanded uncertainties for adiabatic compressibility were determined by combining the associated uncertainties for density and speed of sound in quadrature. The bulk modulus (E_v) of the fuel is given by the following relationship

$$E_v = \kappa_s^{-1} = \rho w^2 \tag{4}$$

and can be calculated from data in Table 2. Changes in the bulk modulus of the fuel can affect the fuel injection timing and amount of nitrogen oxides (NO_x) formed during combustion in a diesel engine.[64]

The results shown in Table 2 are plotted as a function of temperature in Figures 2 and 3 for density and speed of sound, respectively. For comparison, data reported by Prak et al. made using the same model of commercial density and sound speed analyzer have been included in Figures 2 and 3.[16] Figures 2 and 3 also show density data for HRD-76 fuel measured with a Stabinger viscometer,[16] as well as hydrotreated vegetable and algae oil fuels similar in composition.[9] The measurements agree within reported uncertainties, as seen in Figure 4 where the relative deviations of the Prak et al.[16] measurements from the values reported in Table 2 are plotted as a function of temperature. This study expands the measurement range of HRD-76 fuel density down to 5 °C, and the range of speed of sound measurements up to 70 °C.

3.3. Composition and Boiling Temperature As a Function of Distillate Volume Fraction. For the ADC method, we typically record the temperatures at which we visually observe (a) the onset of bubbling, (b) sustained bubbling, and (c) the rise of vapor into the distillation head. While the onset of bubbling and sustained bubbling temperatures are useful as diagnostics during distillation, the vapor rise temperature is the theoretically significant initial boiling temperature (IBT) of the complex fluid. This temperature is important because the sample composition in the boiling flask

is fixed and measurable at the start of the distillation; therefore, the data can be used to develop an equation of state. The measured IBT of HRD-76 is 254.0 °C with a combined uncertainty of 2.6 °C at 83.4 kPa. Using the modified Sydney Young equation to account for ambient pressure, the equivalent IBT at sea-level (101.3 kPa) is 261.7 °C.[65] A fourth-order polynomial linear regression curve was fitted to the measured temperature values over the full distillate volume fraction range

$$T_k \text{ (in °C)} = 260.8 + 1.294V - 0.021286V^2 + 0.00012926V^3 \tag{5}$$

where V is % distillate volume fraction. The uncertainties in the coefficients are 1.06, 0.11, 0.00281, and 1.98×10^{-5}, respectively, at the 95% confidence interval. Equation 5 is used to interpolate boiling temperatures at discrete distillate volume fraction intervals (Table 3).

Figure 5 illustrates the change in the distillate composition measured over the range of the distillation curve. Most of the linear and branched alkanes lighter than dodecane are present in the first two aliquots and are substantially absent in distillate fractions greater than 20% (volume/volume). The changes in distillate composition are consistent with the change in the slope of the distillation curve at the same distillate volume fraction (Figure 6).

The distillate gas chromatograms show rapid volatilization of aliphatic hydrocarbons lighter than tridecane below 280 °C (287 °C at sea-level) near the start of the distillation. The change in composition is important in the formulation of fuel surrogate mixtures that match the distillation curve of HRD-76 fuel.

A recurring pattern of chromatogram peaks produced through the hydroisomerization of n-alkanes can be seen in Figures 1 and 5 under the conditions discussed earlier: double branch isomers elute before single branch isomers, followed by their corresponding n-alkane (see Table S1, Supporting

Table 3. Boiling Temperature (T_k) as a Function of Distillate Volume Fraction (V) for HRD-76 Fuel at 83.4 kPa (with an expanded uncertainty of 0.2 kPa)^a

	pressure, 83.4 kPa $U_c(P) = 0.2$ kPa		pressure, 101.3 kPa
V, % (v/v)	T_k, °C	U_c (T_k), °C	$T_{k,SY}$, °C
5	266.8	0.3	274.7
10	271.7	0.3	279.7
15	275.9	0.3	283.9
20	279.2	0.5	287.3
25	281.9	0.5	290.0
30	284.0	0.6	292.1
35	285.6	0.5	293.7
40	286.8	0.5	295.0
45	287.7	0.5	295.9
50	288.4	0.5	296.7
55	289.1	0.5	297.3
60	289.7	0.6	298.0
65	290.5	0.6	298.7
70	291.4	0.6	299.7
75	292.6	0.5	300.9
80	294.3	0.4	302.6
85	296.4	0.4	304.7
90	299.1	0.6	307.5

^{a}Equivalent temperatures ($T_{k,SY}$) at 101.3 kPa, calculated using the modified Sydney Young equation, are provided for convenience. Combined expanded uncertainty (U_c) values with a coverage factor of 2 are shown to the right of their respective measured values.

Information for further details). The degree of branching in alkane isomers has a strong effect on their normal boiling temperature, which results in a significant difference in their retention time on a nonpolar GC column. The correlation between the normal boiling temperature from the NIST/TRC Web Thermo Tables[66] and the programmed temperature retention index is shown in Figure 7. This relationship may be helpful in confirming the identity of unknown single branch alkanes in other second-generation renewable fuel samples when combined with mass fragmentation pattern data from the NIST 11 Mass Spectral Library.[57]

3.4. Composite Enthalpy of Combustion, Density and Speed of Sound. The ADC composition data can be used to estimate composite thermophysical properties based on the contribution of individual components (see Supporting Information, section S2, for additional details). The composite property estimate approach is particularly useful where the fluid composition is known, but the sample volume is too small for direct measurement of thermophysical properties. Recent improvements in analytical instrumentation[67] and thermophysical data accessibility[68] make composite property estimation an increasingly promising tool in complex fluid analysis. We applied this approach to a composite North American petroleum sample in an earlier work and calculated its density, index of refraction, and average molecular mass as a function of distillate volume fraction. Using these estimates and an empirical model of sulfur content based solely on thermophysical parameters,[63] we concluded that the estimated values of density and sulfur content were consistent with experimentally measured values.[69] Fluid properties estimation from composition is important for bench-scale renewable fuel synthesis and process optimization. Here, we apply the approach to the analysis of bulk HRD-76 fuel and its distillate fractions to

estimate changes in enthalpy of combustion, density, and speed of sound as a function of changes in fluid composition (see Table 4). Additionally, the composite adiabatic compressibility and bulk modulus of HRD-76 can be calculated from the data in Table 4 using eqs 3 and 4, respectively.

The composition of the HRD-76 fuel is well-suited for composite property analysis because it contains fewer and simpler compounds when compared with petroleum-based fuel samples. GC-MS composition data of distillate fractions over three replicate distillations of HRD-76 were used as the basis for composite property calculation. Critically evaluated values from the NIST/TRC Web Thermo Tables were used for individual components to the extent permitted by the standard reference database.[66] Quantitative structure property relationship models or statistical estimates were used in instances where no datum is available for a given compound or when the identity of the alkane isomer could not be fully resolved. For instance, the Cardozo model was used to estimate the enthalpy of combustion,[70] and the Ozerenko model was used to estimate the speed of sound when necessary.[71] Contributions to composite properties from mixing are assumed to be smaller than the uncertainty in the complex fluid composition and the uncertainty in the measured or estimated value of the individual component (see Supporting Information, section S3 for additional details).

Figure 8 shows changes in the composite enthalpy of combustion as a function of distillate volume fraction. The increase in the enthalpy of combustion decreases sharply around 20% (volume/volume) in a manner similar to the distillation curve. There is considerable variability in the composition of early distillate samples, which is reflected by the scatter in composite enthalpy of combustion values less than 20% (volume/volume). The distillate composition and composite thermophysical values past the midpoint of the distillation curve are more repeatable.

Table 4 summarizes the composite enthalpy of combustion, density, and speed of sound values for HRD-76 fuel as a function of distillate volume fraction. The combined expanded uncertainties of the bulk composite properties are approximately 5% of the calculated values. The composite values for fuel density and speed of sound in the HRD-76 fuel are lower than bulk fluid values measured with the density and sound speed analyzer; however, the differences in the two values are not statistically significant at a 95% confidence interval: 744 kg/m^3 composite bulk density with an expanded uncertainty of 38 kg/m^3 compared with 776.93 kg/m^3 measured bulk density with an expanded uncertainty of 0.3 kg/m^3 at 20 °C, and 1301 m/s composite speed of sound with an expanded uncertainty of 64 m/s compared with 1341.8 m/s measured speed of sound with an expanded uncertainty of 1.2 m/s. The composite thermophysical properties approach appears promising and may be used to estimate other parameters for HRD-76 fuel and other second-generation renewable fuels under higher pressures and temperatures.

3.5. Calculated Cetane Index of Bulk HRD-76 Fuel. The fuel ignition quality, as measured by its cetane number (CN) and low-temperature properties, are both strongly affected by the ratio of n-alkanes to branched alkanes in a diesel fuel. The cetane number of a diesel fuel is a measure of its compression ignition quality. Two reference fuels, pure n-hexadecane (cetane) and 2,2,4,4,6,8,8-heptamethylnonane (isocetane), are assigned cetane numbers of 100 and 15, respectively. A test engine is used to compare the compression ignition delay of the
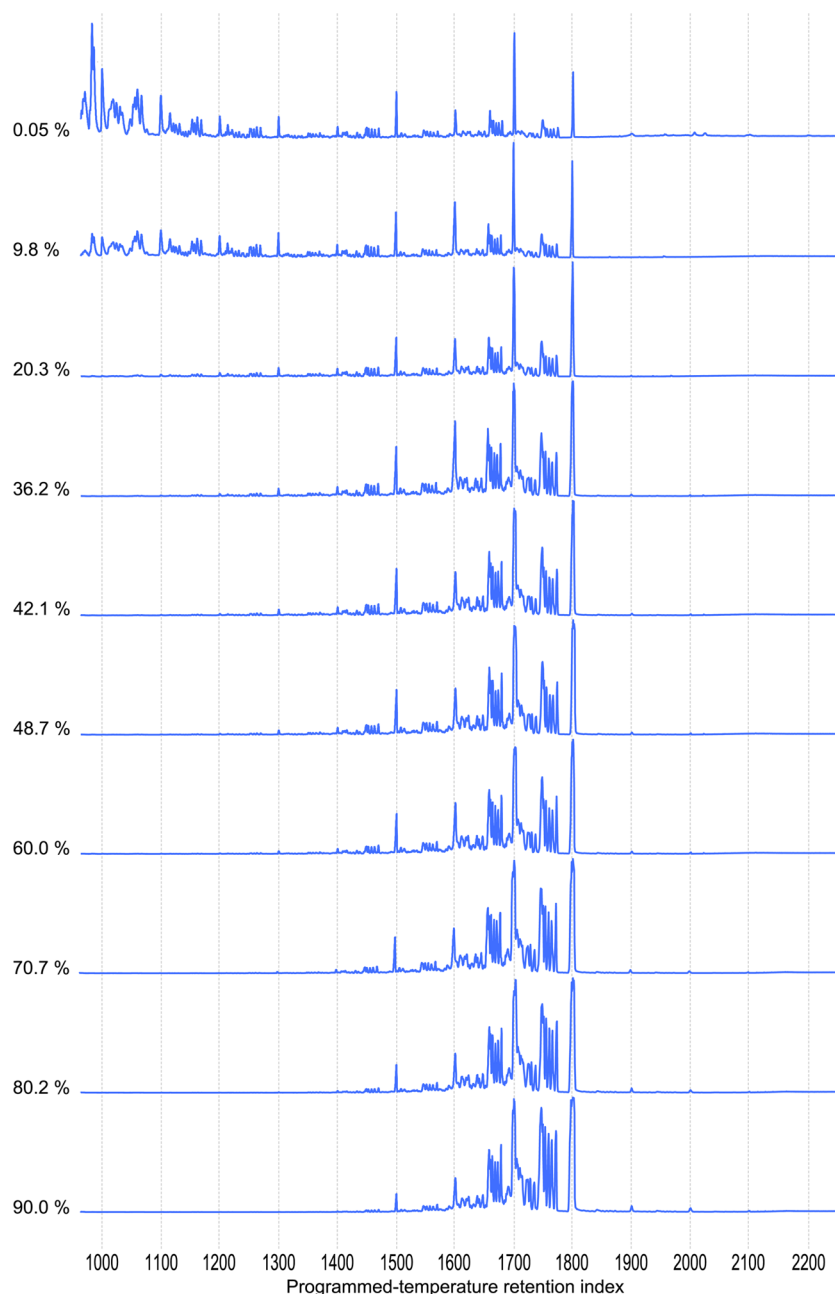
Figure 5. Composition of HRD-76 fuel fractions plotted as a function of programmed-temperature retention index, with distillate volume fraction reported to the left of respective chromatograms in % (volume/volume). The chromatogram intensity reflects the total ion current as a function of the programmed-temperature retention index (I^T). The I^T values are calculated from n-alkanes present in each distillate sample.

diesel fuel with reference fuel blends.[11] The calculated cetane index (CCI), based on the boiling temperatures at 10%, 50%, and 90% distillate volume fraction and the diesel fuel density, is often used to estimate the cetane number when a test engine is not available or when the sample volume is too small for engine testing.[72] The CN can also be derived from the ignition delay in an ignition quality tester.[11] We used the measured density and distillation curve of HRD-76 fuel to determine its CCI with the four-variable equation specified in ASTM D4737 (see Supporting Information, section S4 for additional details).[68] Table 5 summarizes the thermophysical data (e.g., boiling points as a function of distillate volume fraction and density) and CCI for HRD-76 fuel, along with CCI, derived CN, and cloud points for two hydrotreated renewable fuels based on

algal oil and vegetable oil with similar compositions.[9] The CCI values and cloud point of the three fuels are similar.

Bezaire et al. noted a statistically significant difference between CCI and derived CN for first-generation biodiesel fuel and synthetic paraffinic kerosene; in contrast, ultralow sulfur diesel fuel and petroleum-based JP-8 jet fuel showed no significant differences between CCI and derived CN.[73] A comparison of CCI and derived CN values based on published data for second-generation renewable fuels shows that the coefficients in the ASTM D4737 four-variable equation produce CCI values that differ significantly when compared with derived CN values (Figure 9) by 9 to 16.[9] The differences in composition between petroleum-based diesel fuels and second-generation renewable fuels and F-T synthetic fuels may
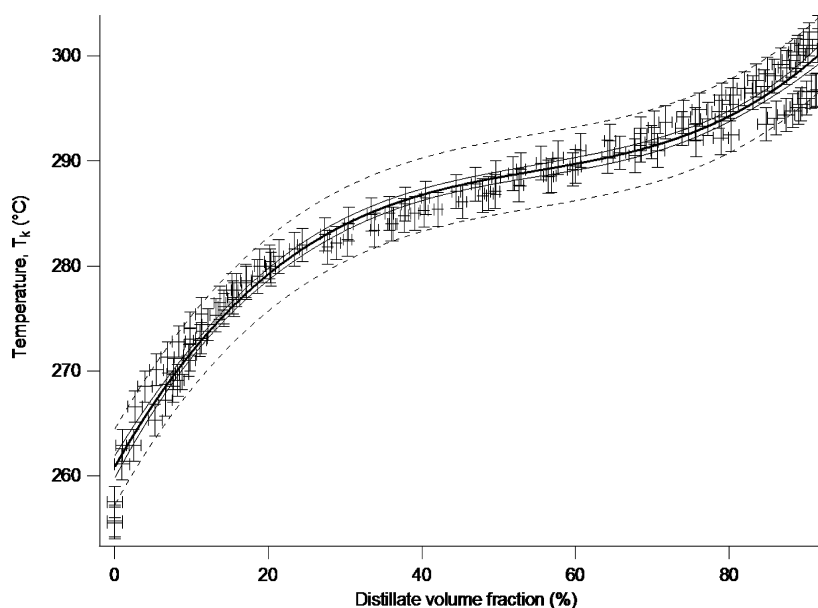
Figure 6. Distillation curve data for an algae-based hydrotreated renewable diesel fuel (HRD-76) at 83.4 kPa (with an expanded uncertainty of 0.2 kPa). A fourth-order polynomial linear regression curve (thick black line), 95% confidence interval (—) and 95% prediction interval (--) are also plotted for comparison. See text for a discussion of uncertainties in the measurement results.
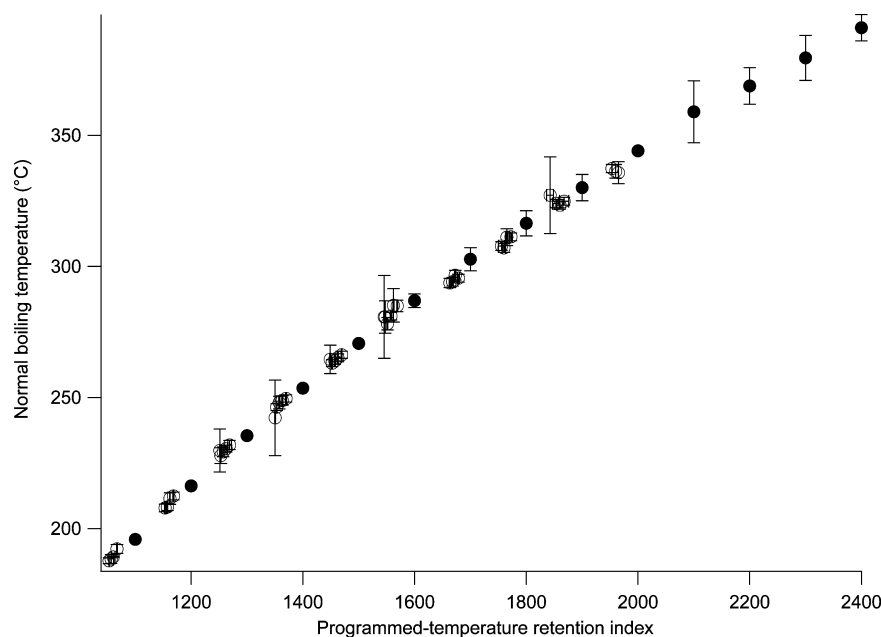

Figure 7. The normal boiling temperature of n-alkanes (●) and single branch alkanes (○) plotted as a function of their average programmed-temperature retention index. Error bar show the expanded uncertainty with a coverage factor of 2. Three or more replicate measurements were made for each single branch alkane compound.

be sufficiently large to justify revising the parameters in the CCI equation for these fuels.

O'Connor et al. noted the inadequacy of the ASTM D4737 four-variable equation, based on density and boiling point data, in calculating the CN of F-T diesel fuels.[74] A composition-based approach, based on the ratio between CH_2 and CH_3 carbons, was recommended in its place. The CH_2/CH_3 ratio of HRD-76 fuel is 3.62, based on ^{13}C NMR data measured in this study. The ratio translates to an estimated CN of 86.9 for the HRD-76 fuel. The value is possibly higher than the derived CN values reported for fuels of similar composition because the O'Connor model works best for diesel fuels with CN ranging

from 29 to 52. Due to the similarity in composition of second-generation renewable fuels and F-T synthetic fuels, the composition-based approach may provide CN estimates closer to derived CN measured through ignition-quality testing when compared with CCI values based on density and boiling points values.

3.6. Cloud Point of Bulk HRD-76 Fuel. The cloud point, or temperature at which paraffinic wax precipitates in a diesel fuel, is an important fuel property. The precipitation of a solid n-alkane crystalline phase can thicken the fuel and clog filters.[75] The formation of the wax crystals can be detected optically through light scattering. The cloud point of HRD-76 fuel was

Table 4. Composite Enthalpy of Combustion ($\Delta H_c{}^\circ$), Density (ρ), and Speed of Sound (w) as a Function of Distillate Volume Fraction (V) for HRD-76 Fuel Based on Three Replicate Distillations[a]

V, % (v/v)	$U(V)$, %	$\Delta H_c{}^\circ$, kJ/mol	U_c ($\Delta H_c{}^\circ$), kJ/mol	ρ, kg/m^3	U_c (ρ), kg/m^3	w, m/s	U_c (w), m/s
0.1	0.1	−7222	1206	744	15	1247	33
9.8	1.3	−8283	833	757	9	1273	19
20.3	1.1	−9839	355	773	4	1302	11
30.4	0.7	−9975	201	774	3	1304	10
40.0	1.7	−10 173	179	776	4	1307	11
49.3	1.3	−10 353	219	777	5	1308	12
60.1	1.4	−10 409	36	777	4	1310	11
70.3	1.4	−10 506	24	778	5	1311	12
80.3	1.5	−10 605	46	779	5	1311	12
90.0	1.8	−10 733	75	780	6	1312	13
residue		−10 950	39	781	5	1312	13
bulk		−9991	500	744	38	1301	64

[a]Composite properties are based on weighted average values of critically evaluated component values at 20 °C. Combined expanded uncertainty (U_c) values with a coverage factor of 2 are shown to the right of their respective measured values.
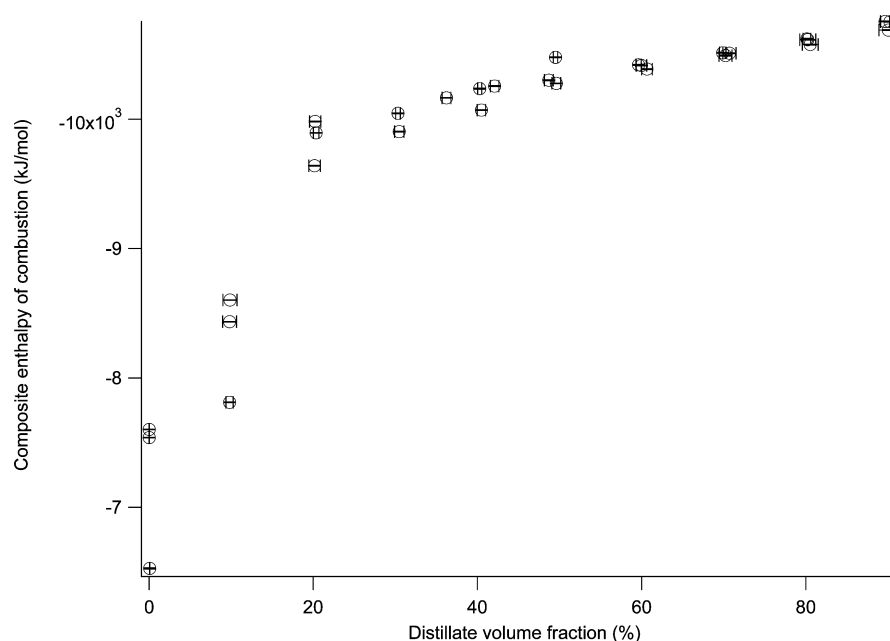

Figure 8. Composite enthalpy of combustion plotted as a function of distillate volume fraction. Error bars show the expanded uncertainty with a coverage factor of 2; the uncertainty values for the enthalpy of combustion are smaller than the plotting symbol.

Table 5. Selected Distillation Points, Calculated Cetane Index and Cloud Point Values for HRD-76 Fuel and Two Hydrotreated Renewable Diesel Fuels with Similar Compositions and Distillation Temperatures[a]

	ASTM method	units	HRD-76 fuel	U_c	hydrotreated algal oil[9]	hydrotreated vegetable oil[9]
initial boiling point		°C	261.7	2.6	183	156
T10		°C	279.7	0.3	249	226
T50		°C	296.7	0.5	280	278
T90		°C	307.5	0.6	293	293
density at 15 °C		kg/m^3	780.38	0. 31	781.6	776.6
calculated cetane index	D4737		101.2	1.0	98.7	99.1
derived cetane number	D6890				78.8	81.4
cloud point	D5773	°C	−6.6	0.6	−5.0	−5.0

[a]Combined expanded uncertainty (U_c) values with a coverage factor of 2 are shown to the right of their respective measured values. See text for discussion of uncertainty in measurement results.

measured using a modified constant cooling rate method, in which Peltier cooling is replaced with air-cooling in a temperature-controlled environmental chamber. Figure 10 is a representative plot of scattered light intensity as a function of

temperature for the HRD-76. The cloud point corresponds to the temperature at which the growing paraffin wax crystals begin scattering the incident light. An increase in the scattered light intensity from the baseline marks the transition region.
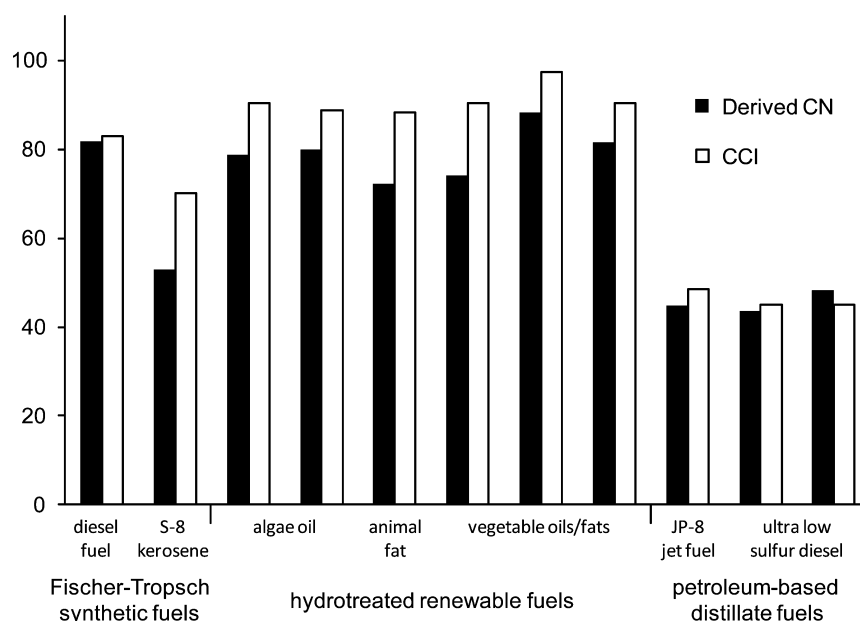
Figure 9. Derived cetane number (CN) and calculated cetane index (CCI) values for Fischer–Tropsch (F-T) synthetic fuels, hydrotreated renewable fuels and petroleum-based distillate fuels from Smagala et al.[9] and Bezaire.[73] CCI values calculated from density and boiling temperatures at 10%, 50%, and 90% distillate volume fraction are higher than derived CN values from ignition quality testing in F-T and hydrotreated renewable fuels.
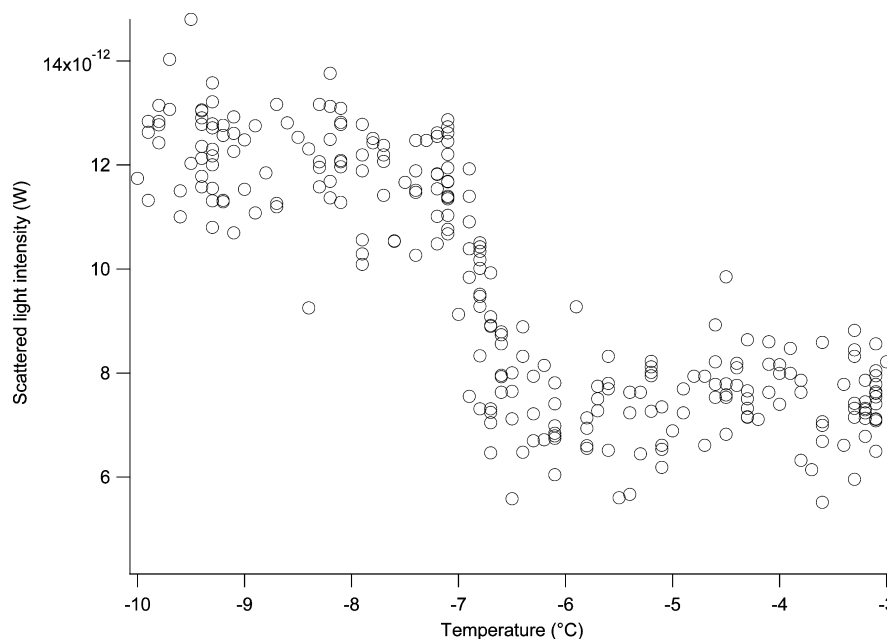

Figure 10. Scattered light intensity plotted as a function of HRD-76 fuel temperature during cooling; uncertainty values are smaller than the plotting symbol.

The cloud point is determined by fitting a regression line to the scattered light intensity in the transition region, and finding its intersection with an average of the scattered light intensity baseline. The cloud point of HRD-76 fuel was found to be −6.6 °C, with an expanded combined uncertainty of 0.6 °C. This is comparable to but slightly lower (by 1.6 °C) than cloud points of similar hydrotreated renewable diesel fuels.[9]

The effect of evaporation on fluid composition, and increase in the measured cloud point, was examined by repeating the experiment on the same sample over several days. Figure 11 shows the increase in measured cloud point of HRD-76 fuel

due to evaporation of volatile compounds. The change in composition through selective removal of lower molecular mass compounds results in the relative enrichment of heavy *n*-alkanes in the HRD-76 fuel. The same effect may be achieved by adjusting the hydroisomerization process parameters to change the linear to branched alkane ratio to favor *n*-alkanes during fuel processing.

4. CONCLUSIONS

We analyzed a sample of HRD-76 fuel using the ADC method and measured its boiling temperature as a function of distillate
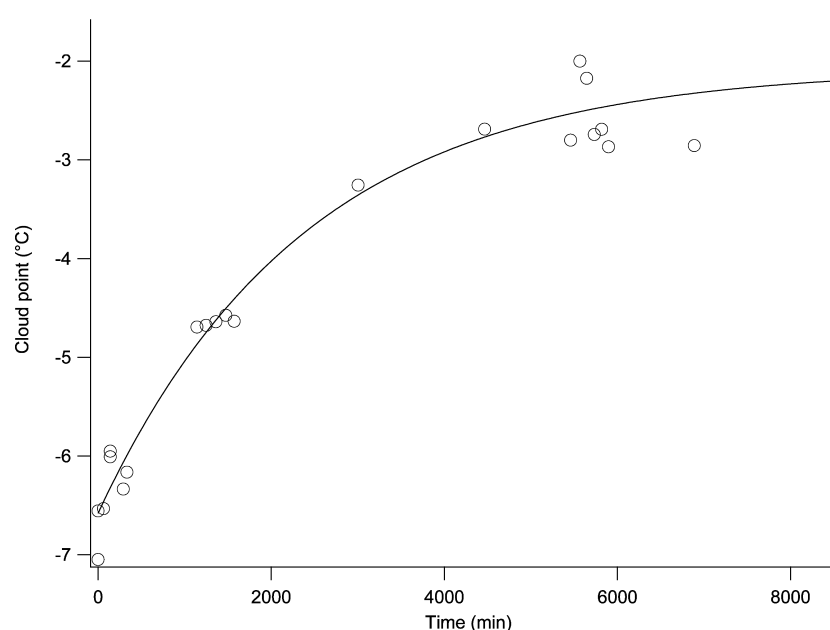
Figure 11. Cloud point plotted as a function of time; uncertainty values are smaller than the plotting symbol. The increase in the cloud point is attributable to the change in HRD-76 fuel composition due to evaporation of volatile compounds over time.

volume fraction. The compositions of the distillate and bulk fluid were determined through NMR spectroscopy and GC-MS analysis. The bulk HRD-76 fuel was found to contain principally linear and lightly branched alkanes containing 14–18 carbon atoms. Differences in the CH, CH_2, and CH_3 carbon ratios based on NMR and GC-MS data were found to be statistically insignificant. Composite enthalpy of combustion, density, and speed of sound values for bulk HRD-76 fuel and its distillate fractions were calculated using composition and a combination of critically evaluated thermophysical properties and quantitative structure property relationship models. The composite density and speed of sound values of the bulk fluid were within 5% of bulk fluid values measured with a density and sound speed analyzer.

The cetane index of the HRD-76 fuel was calculated from its density and boiling temperatures at 10%, 50%, and 90% distillate volume fraction. The CCI of HRD-76 is 101.2, with a combined expanded uncertainty of 1.0, and is comparable to published values for F-T fuels and hydrotreated renewable fuels. Literature CCI values for F-T fuels and hydrotreated renewable fuels appear to be systematically higher than derived cetane numbers for the same fuels measured in an ignition-quality tester. The cetane number of HRD-76 was also estimated using ^{13}C NMR composition data and was found to be closer to the derived cetane numbers for hydrotreated renewable diesel fuels with similar compositions. The cloud point of HRD-76 was found to be slightly lower (by 1.6 °C) compared with the published values of similar hydrotreated renewable diesel fuels.

This work provides the thermophysical and chemical data needed to model changes in HRD-76 fuel properties as a function of composition. Furthermore, it shows that NMR and GC-MS compositional data can be coupled with critically evaluated thermodynamic data and quantitative structure property relationship models to estimate fluid properties such as enthalpy of combustion, density and speed of sound with reasonable accuracy. In addition, it suggests that the calculated cetane index based on density and boiling temperatures

overestimates the cetane number of F-T and hydrotreated renewable diesel fuels. The data presented in Tables 2, 3, and 4, along with the IBT of HRD-76, may used to develop equations of state for second-generation hydrotreated renewable distillate fuels. The composition data of HRD-76, shown in Figures 1 and 5 and enumerated in Supporting Information, section S1, can be used to aid the development of surrogate fuel mixtures for aliphatic renewable or synthetic fuels.

■ ASSOCIATED CONTENT

ⓢ Supporting Information

S1. Use of programmed-temperature retention indices to assist in peak identification. S2. Calculation of composite thermophysical properties. Table S1. Programmed temperature retention indices (I^T) of linear and branched alkanes present in HRD-76 fuel. Table S2. Enthalpy of combustion (ΔH_c°), density (ρ) at 20 °C, and speed of sound (w) of linear and branched alkanes identified in the HRD-76 fuel at 20 °C. S3. Excess molar properties and measurement uncertainty. S4. Calculated cetane indices of hydrotreated renewable fuels. This material is available free of charge via the Internet at http://pubs.acs.org.

■ AUTHOR INFORMATION

Corresponding Author

*Phone: 1-303-497-5158. Fax: 1-303-497-6682. E-mail: bruno@boulder.nist.gov.

Notes

The authors declare no competing financial interest.

■ ACKNOWLEDGMENTS

■ ABBREVIATIONS AND ACRONYMS

ADC = advanced distillation curve

ASTM = ASTM International (formerly American Society for Testing and Materials)
CCI = calculated cetane index
CN = cetane number
DEPT = distortionless enhancement by polarization transfer
DSA = density and speed of sound analyzer
FAME = fatty acid methyl esters
F-T = Fischer–Tropsch
GC-MS = gas chromatography with mass spectrometric detection
HRD-76 = hydrotreated renewable distillate (or diesel) fuel, F-76 grade
IBT = initial boiling temperature
k = coverage factor
NIST = National Institute of Standards and Technology
NMR = nuclear magnetic resonance spectroscopy
NO_x = nitrogen oxides
SY = Sydney Young
SRM = standard reference material
SVM = Stabinger viscometer
T_h = headspace temperature
T_k = fluid temperature

■ REFERENCES

(1) Agarwal, A. K. *Prog. Energy Combust. Sci.* **2007**, *33*, 233.
(2) Rosenthal, E. Rush to use crops as fuel raises food prices and hunger fears; *New York Times*, April 7, 2011; p A1.
(3) Sims, R. E. H.; Mabee, W.; Saddler, J. N.; Taylor, M. *Bioresour. Technol.* **2010**, *101*, 1570.
(4) Surisetty, V. R.; Dalai, A. K.; Kozinski, J. *Appl. Catal., A* **2011**, *404*, 1.
(5) Arisoy, K. *Energy Sources Part A* **2008**, *30*, 1516.
(6) Willauer, H. D.; Mushrush, G. W.; Bauserman, J. W.; Williams, F. W. *Synthetic Fuels and Biofuels: Questionable Replacements for Petroleum*; Naval Research Laboratory: Washington, DC, 2008.
(7) Schenk, P.; Thomas-Hall, S.; Stephens, E.; Marx, U.; Mussgnug, J.; Posten, C.; Kruse, O.; Hankamer, B. *Bioenerg. Res.* **2008**, *1*, 20.
(8) Sheehan, J.; Dunahay, T.; Benemann, J.; Roessler, P. *A Look Back at the U.S. Department of Energy's Aquatic Species Program - Biodiesel from Algae*; National Renewable Energy Laboratory: Golden, CO, 1998.
(9) Smagala, T. G.; Christensen, E.; Christison, K. M.; Mohler, R. E.; Gjersing, E.; McCormick, R. L. *Energy Fuels* **2013**, *27*, 237.
(10) Robota, H. J.; Alger, J. C.; Shafer, L. *Energy Fuels* **2013**, *27*, 985.
(11) Murphy, M. J.; Taylor, J. D.; McCormick, R. L. *Compendium of Experimental Cetane Number Data*; National Renewable Energy Laboratory: Golden, CO, 2004.
(12) Al-Sabawi, M.; Chen, J. *Energy Fuels* **2012**, *26*, 5373.
(13) Kasza, T.; Solymosi, P.; Varga, Z.; Horath, I. W.; Hancsok, J. *Chem. Eng. Trans.* **2011**, *24*, 1519.
(14) Lee, C. S.; Park, S. W.; Kwon, S. I. *Energy Fuels* **2005**, *19*, 2201.
(15) Leckel, D. *Energy Fuels* **2009**, *23*, 2342.
(16) Prak, D. J. L.; Trulove, P. C.; Cowart, J. S. *J. Chem. Eng. Data* **2013**, *58*, 920.
(17) Bruno, T. J.; Ott, L. S.; Smith, B. L.; Lovestead, T. M. *Anal. Chem.* **2010**, *82*, 777.
(18) Bruno, T. J.; Ott, L. S.; Lovestead, T. M.; Huber, M. L. *Chem. Eng. Technol.* **2010**, *33*, 363.
(19) Bruno, T. J.; Ott, L. S.; Lovestead, T. M.; Huber, M. L. *J. Chromatogr., A* **2010**, *1217*, 2703.
(20) Bruno, T. J. *Ind. Eng. Chem. Res.* **2006**, *45*, 4371.
(21) Hadler, A. B.; Ott, L. S.; Bruno, T. J. *Fluid Phase Equilib.* **2009**, *281*, 49.
(22) Bruno, T. J.; Smith, B. L. *Ind. Eng. Chem. Res.* **2006**, *45*, 4381.
(23) Smith, B. L.; Bruno, T. J. *Energy Fuels* **2007**, *21*, 2853.
(24) Smith, B. L.; Bruno, T. J. *Ind. Eng. Chem. Res.* **2007**, *46*, 310.
(25) Smith, B. L.; Bruno, T. J. *J. Propul. Power* **2008**, *24*, 618.
(26) Bruno, T. J.; Baibourine, E.; Lovestead, T. M. *Energy Fuels* **2010**, *24*, 3049.
(27) Burger, J. L.; Bruno, T. J. *Energy Fuels* **2012**, *26*, 3661.
(28) Ott, L. S.; Smith, B. L.; Bruno, T. J. *Energy Fuels* **2008**, *22*, 2518.
(29) Ott, L. S.; Bruno, T. J. *Energy Fuels* **2008**, *22*, 2861.
(30) Smith, B. L.; Ott, L. S.; Bruno, T. J. *Environ. Sci. Technol.* **2008**, *42*, 7682.
(31) Smith, B. L.; Ott, L. S.; Bruno, T. J. *Ind. Eng. Chem. Res.* **2008**, *47*, 5832.
(32) Bruno, T. J.; Wolk, A.; Naydich, A.; Huber, M. L. *Energy Fuels* **2009**, *23*, 3989.
(33) Windom, B. C.; Lovestead, T. M.; Mascal, M.; Nikitin, E. B.; Bruno, T. J. *Energy Fuels* **2011**, *25*, 1878.
(34) Hsieh, P. Y.; Abel, K. R.; Bruno, T. J. *Energy Fuels* **2013**, *27*, 804.
(35) Smith, B. L.; Bruno, T. J. *Ind. Eng. Chem. Res.* **2007**, *46*, 297.
(36) Bruno, T. J.; Wolk, A.; Naydich, A. *Energy Fuels* **2009**, *23*, 2295.
(37) Bruno, T. J.; Wolk, A.; Naydich, A. *Energy Fuels* **2009**, *23*, 3277.
(38) Ott, L. S.; Hadler, A. B.; Bruno, T. J. *Ind. Eng. Chem. Res.* **2008**, *47*, 9225.
(39) Lovestead, T. M.; Bruno, T. J. *Energy Fuels* **2009**, *23*, 3637.
(40) Lovestead, T. M.; Windom, B. C.; Riggs, J. R.; Nickell, C.; Bruno, T. J. *Energy Fuels* **2010**, *24*, 5611.
(41) Ott, L. S.; Bruno, T. J. *Energy Fuels* **2007**, *21*, 2778.
(42) Ott, L. S.; Bruno, T. J. *J. Sulfur Chem.* **2007**, *28*, 493.
(43) Ott, L. S.; Smith, B. L.; Bruno, T. J. *Fuel* **2008**, *87*, 3379.
(44) Ott, L. S.; Smith, B. L.; Bruno, T. J. *Fuel* **2008**, *87*, 3055.
(45) Huber, M. L.; Smith, B. L.; Ott, L. S.; Bruno, T. J. *Energy Fuels* **2008**, *22*, 1104.
(46) Huber, M. L.; Lemmon, E. W.; Diky, V.; Smith, B. L.; Bruno, T. J. *Energy Fuels* **2008**, *22*, 3249.
(47) Huber, A. L.; Lemmon, E. W.; Ott, L. S.; Bruno, T. J. *Energy Fuels* **2009**, *23*, 3083.
(48) Bruno, T. J.; Huber, M. L. *Energy Fuels* **2010**, *24*, 4277.
(49) Huber, M. L.; Lemmon, E. W.; Bruno, T. J. *Energy Fuels* **2010**, *24*, 3565.
(50) Mueller, C. J.; Cannella, W. J.; Bruno, T. J.; Bunting, B.; Dettman, H. D.; Franz, J. A.; Huber, M. L.; Natarajan, M.; Pitz, W. J.; Ratcliff, M. A.; Wright, K. *Energy Fuels* **2012**, *26*, 3284.
(51) Huber, M. L.; Lemmon, E. W.; Bruno, T. J. *Energy Fuels* **2009**, *23*, 5550.
(52) Huber, M. L.; Lemmon, E. W.; Kazakov, A.; Ott, L. S.; Bruno, T. J. *Energy Fuels* **2009**, *23*, 3790.
(53) Bruno, T. J.; Smith, B. L. *Energy Fuels* **2010**, *24*, 4266.
(54) Windom, B. C.; Huber, M. L.; Bruno, T. J.; Lown, A. L.; Lira, C. T. *Energy Fuels* **2012**, *26*, 1787.
(55) Windom, B. C.; Bruno, T. J. *Ind. Eng. Chem. Res.* **2011**, *50*, 1115.
(56) Bruno, T. J.; Svoronos, P. D. N. *Handbook of Basic Tables for Chemical Analysis*, 3rd ed.; Taylor & Francis: Boca Raton, 2011.
(57) Stein, S. E.; Babushok, V. I.; Brown, R. L.; Linstrom, P. J. *J. Chem. Inf. Model.* **2007**, *47*, 975.
(58) Petrakis, L.; Allen, D. *NMR for Liquid Fossil Fuels*; Elsevier: Amsterdam, 1987.
(59) Fortin, T. J.; Laesecke, A.; Freund, M.; Outcalt, S. *J. Chem. Thermodyn.* **2013**, *57*, 276.
(60) Laesecke, A.; Fortin, T. J.; Splett, J. D. *Energy Fuels* **2012**, *26*, 1844.
(61) Whetstone, J. R.; Trahey, N. M. *Certificate of Analysis — Standard Reference Material 211d*; National Institute of Standards and Technology: Gaithersburg, MD, 2009.
(62) Standard test method for cloud point of petroleum products (constant cooling rate method), ASTM Standard D5773-10, *Book of Standards*; ASTM International: West Conshohocken, PA, 2010.
(63) Riazi, M. R. *Characterization and Properties of Petroleum Fractions*; ASTM International: West Conshohocken, PA, 2005.
(64) Boehman, A. L.; Morris, D.; Szybist, J.; Esen, E. *Energy Fuels* **2004**, *18*, 1877.
(65) Ott, L. S.; Smith, B. L.; Bruno, T. J. *J. Chem. Thermodyn.* **2008**, *40*, 1352.

(66) Kazakov, A. F.; Muzny, C. D.; Chirico, R. D.; Diky, V.; Frenkel, M. *NIST/TRC Web Thermo Tables*, 2-2012-1-Pro ed.; NIST Standard Reference Database 203; National Institute of Standards and Technology: Gaithersburg, MD, 2012.

(67) Marshall, A. G.; Rodgers, R. P. *Proc. Natl. Acad. Sci. U. S. A.* **2008**, *105*, 18090.

(68) Diky, V.; Muzny, C. D.; Lemmon, E. W.; Chirico, R. D.; Frenkel, M. *J. Chem. Inf. Model.* **2007**, *47*, 1713.

(69) Hsieh, P. Y.; Bruno, T. J. *Energy Fuels* **2014**, *28*, 1868.

(70) Cardozo, R. L. *AIChE J.* **1986**, *32*, 844.

(71) Ozerenko, A. A.; Gyul'maliev, A. M.; Gagarin, S. G. *Coke Chem.* **2007**, *50*, 392.

(72) Standard test method for calculated cetane index by four variable equation, ASTM Standard D4737-10; *Book of Standards*; ASTM International: West Conshohocken, PA, 2010.

(73) Bezaire, N.; Wadumesthrige, K.; Ng, K. Y. S.; Salley, S. O. *Fuel* **2010**, *89*, 3807.

(74) O'Connor, C. T.; Forrester, R. D.; Scurrell, M. S. *Fuel* **1992**, *71*, 1323.

(75) Coutinho, J. A. P.; Mirante, F.; Ribeiro, J. C.; Sansot, J. M.; Daridon, J. L. *Fuel* **2002**, *81*, 963.